Low-Frequency Tremors Immediately After the 2011 Tohoku-Oki Earthquake Detected by Near-Trench OBS Observations

Hidenobu Takahashi (hidenobu@dc.tohoku.ac.jp)
Tohoku Daigaku https://orcid.org/0000-0002-3938-4721
Ryota Hino
Tohoku University: Tohoku Daigaku
Naoki Uchida
Tohoku University: Tohoku Daigaku
Takanori Matsuzawa
National Research Institute for Earth Science and Disaster Resilience
Yusaku Ohta
Tohoku University: Tohoku Daigaku
Syuichi Suzuki
Tohoku University: Tohoku Daigaku
Masanao Shinohara
Tokyo University

Express Letter

Keywords: Tectonic tremor, Ocean bottom seismometer, The 2011 off the Pacific coast of Tohoku earthquake, slow earthquake, aseismic slip

Posted Date: October 12th, 2020

DOI: https://doi.org/10.21203/rs.3.rs-89488/v1

Abstract

We used temporal seismic observation using pop-up type ocean-bottom seismometers to detect a number of low-frequency tremors (LFTs) immediately after the 2011 Tohoku-Oki earthquake in the northern periphery of its aftershock area. The near-field observation clearly distinguished LFTs from regular earthquakes based on their spectral shape in the frequency band of 1–4 Hz. In addition to the LFTs accompanied by known very low frequency earthquakes (VLFEs), more than 130 LFTs without known VLFE activity were detected during April–October, 2011. The newly detected LFTs were in the vicinity of a sequence of small repeating earthquakes indicating mixed distribution of LFTs and regular interplate earthquakes in the region. The LFTs and repeating earthquake activities show a periodicity of 60–100 days, which is similar to that of the LFT activity in the later period (2016–2018). This suggests that the LFT activity is modulated by sustained background aseismic slip events throughout the postseismic period of the 2011 mainshock.

Introduction

Studies have detected various types of slow earthquakes all over the world, and their activity on subduction interfaces is expected to have a strong relationship with the generation processes of massive interplate earthquakes (e.g., Obara and Kato, 2016). Low-frequency tremors (LFTs) are a slow earthquake phenomenon characterized by unclear P- and S-wave arrivals with a dominant frequency of 2–8 Hz and smaller amplitudes than those of regular earthquakes with similar seismic moments. LFTs are usually active at the margins of seismogenic zones, both at the downdip (e.g., Obara, 2002; Frank et al., 2014) and updip (e.g., Obana and Kodaira, 2009; Todd et al., 2018) sides. The simultaneous occurrences of LFTs and other slow earthquakes are often observed. For example, spatiotemporal coincidence of LFTs and very low frequency earthquakes (VLFEs; e.g., Yamashita et al., 2015) and another type of slow earthquake has been observed in the Hyuga-nada region (Yamashita et al., 2015) and the Nankai subduction zone (Kaneko et al., 2018; Toh et al., 2018). Such a relationship between different types of slow earthquake phenomena suggests that this series of different dominant frequencies is a united broadband phenomenon (Ide, 2008; Ide, 2019), and it is important to use as many types of slow earthquakes to detect the broadband phenomenon and their spatiotemporal associations.

Recently, slow earthquakes were detected along the Japan Trench subduction zone that hosted the 2011 Tohoku-Oki earthquake (Mw 9.1). Matsuzawa et al. (2015) identified VLFEs by inspecting onshore broadband seismograms since 2005 and showed that they are concentrated within several small areas based on correlation with manually identified template events. Baba et al. (2020) also used onshore broadband seismograms since 2003 and estimated the distribution of VLFEs by using the waveform correlation with synthetic interplate events. Tanaka et al. (2019) and Nishikawa et al. (2019) detected remarkable LFT activity near the Japan and Kuril trenches that are distributed along the plate-boundary depth of 10–20 km. These discoveries were made possible by the new cabled seafloor observation network for earthquakes and tsunamis along the Japan Trench (S-net) that cover east off NE Japan by 150 seismometers. Knowledge about the activities of LFTs prior to the deployment of the S-net in 2016 is,

however, quite limited in time and space because near-source ocean bottom seismograms (OBSs) are required to detect weak signal radiation. Using temporal OBS observations, Ito et al. (2015) and Katakami et al. (2018) identified the LFT activity for ~ 1.5 months immediately before the 2011 Tohoku-Oki earthquake near its hypocenter. Ohta et al. (2019) reported the LFT activities coexisting with the shallow afterslip of the 2011 earthquake ~ 5 years after the occurrence of the mainshock, from October 2016 to September 2017, in the southern Japan Trench. It is expected that LFTs are occurring more frequently than VLFEs and thus the LFTs are suitable to detect the broadband phenomena. The activity of LFTs in the very early postseismic period after huge interplate earthquakes is of particular interest, as it may allow us to detect more slow earthquake episodes, investigate relationship between slow earthquakes and understand its temporal evolution in the vicinity of the Tohoku-Oki earthquake. However, so far, no detailed studies based on near-source observations have been made for the period.

In this study, we inspected the seismograms obtained by the OBS observations made immediately after the 2011 Tohoku earthquake in the northern Japan Trench, ~ 250 km away from its hypocenter and at the northern rim of the early aftershock distribution. Within the observation period, several VLFEs were located near the OBS array by Matsuzawa et al. (2015), and it is expected that the OBSs detected LFTs associated with the VLFEs. Since the small repeating earthquakes (SREs) were also activated in the area at that time (Uchida and Matsuzawa, 2013), this provides a unique opportunity to investigate the relationship among the LFTs, VLFE, and SREs in the early postseismic period of the massive interplate earthquake in the periphery of its rupture area.

Observations

A total of five free-fall and pop-up type OBSs were deployed at the northern rim of the aftershock area of the 2011 Tohoku-Oki earthquake and observation was made from April 11 to October 25, 2011 (Fig. 1a) to monitor the temporal expansion of the aftershock area immediately after the occurrence of the mainshock. Three-component velocity seismograms from geophones with a natural frequency of 4.5 Hz geophones were recorded at 100 Hz sampling. During the observation, Matsuzawa et al. (2015) identified seven VLFEs located near the OBS array; we call them VLFE #1–7 in the order of their occurrences.

The OBS seismograms around the origin times of the VLFEs show gradual increases in horizontal amplitudes with unclear P- and S-wave arrivals (Figs. 1b and S1). Note that the VLFEs (Mw 3.4–3.6) have peak amplitudes below 0.1 Hz, and they were identified based on the onshore broadband seismograms (Matsuzawa et al., 2015). The timings of the peak amplitudes of the OBS seismograms seem to be delayed as the epicentral distances from the VLFEs increase. The amplitudes decreased in the order of the epicentral distances. The order of the timing of the peak amplitude as well as the spatial decay of the amplitudes resemble those of SREs (Uchida and Matsuzawa, 2013), regular earthquakes on the plate boundary, close to the VLFE epicenters. As an example, the seismograms of an SRE (hereafter SRE-A; M3.9) whose epicenter is closest to VLFE #5 are shown in Fig. 1. Although SRE-A shows much larger amplitude and clearer P- and S-wave onsets than the seismograms at the VLFE timing, the orders of arrival times and of peak amplitudes at different OBSs are similar (Fig. 1). The amplitude variations

among the OBSs are also similar for all the seismograms at the time of the other VLFEs (Figure S2). This characteristic suggests that these recorded signals radiated from sources that are very close to the hypocenter of SRE-A.

Although the source locations of the seven events are expected to be close to SRE-A, seismograms of the newly observed events are significantly different in their frequency contents from that of SRE-A. Figure 1c shows the power spectral density (PSD) of the horizontal records of LFT #5 and that of SRE-A at the station AO.S05, which is nearest to the VLFE #5. The PSD of the events has different decay pattern in the frequency range 1–4 Hz from that of SRE-A. It is confirmed that the other six events associated with the VLFEs also present a similar shape of PSDs (Figure S3).

As high-frequency signals are attenuated because of the path effect, deficits in the high-frequency component can also be identified in the seismograms of remote regular earthquakes. For example, the PSD below 6 Hz of the seismogram of an earthquake of ~ 160 km in the epicentral distance resembles the PSDs of the events identified at the VLFE timings (Figure S3). However, the spatial variation of the observed amplitudes is clearly different from those of the events associated with the VLFEs (Figures S1 and S2). Therefore, we can distinguish local low-frequency events from remote earthquakes. As demonstrated by Toh et al. (2018), amplitude variations at different OBS stations are important for interpreting the locations of low-frequency events.

Based on these observations, the similarity in amplitude variation with a local SRE and the evident deficit of high-frequency energy, we interpret the events detected at the timing of the known VLFEs are seismic waves that radiated from LFTs whose sources are close to those of the VLFEs and the SRE. Hereafter, we call these events LFT #1 to LFT #7 according the number of associating VLFEs.

Searching for additional LFTs

In the previous section, we showed that short-period OBSs deployed near the known VLFE epicenters recorded LFTs associated with the VLFEs. Here, we try to explore undetected LFTs that is not associated with the VLFEs, because it is expected that the frequency of LFTs is more than that of VLFEs (e.g., Ghosh et al., 2015; Ohta et al., 2019; Nishikawa et al., 2019). Based on the similarities of the peak amplitude patterns (Figure S2) and of the PSDs (Figure S3) among the LFTs #1–7, we searched for seismograms having these characteristics. To this end, we quantified these two characteristics. We introduce a quantity termed “Amplitude Index” (AI, Text S1 for detailed explanation) to measure the similarity of the peak amplitude pattern of sampled seismograms with those of LFTs #1–7. AI measures discrepancy between the peak amplitude distribution of samples and the average distribution for the seven LFTs. Sample seismograms were taken from continuous seismograms using a sliding time-window of 30 s with a time interval of 15 s, after applying a band-pass (2–4 Hz) filter, because the signals of LFTs are most pronounced in this frequency band. As a measure of similarity of PSDs, we calculated residual sum of squares (RSS_spectra, Text S1) between a PSD of a sample waveform and the PSD of LFT #5, which was observed with the highest signal-to-noise ratio (S/N). Sample PSDs were calculated from the seismograms extracted using sliding time-windows identical to the AI calculation. RSS_spectra were

calculated in a frequency band of 1–4 Hz. Both AI and RSS_spectra take smaller values when a sampled seismogram resembles more to those of the LFTs.

Figure 2 shows the two-hour spectrograms including for LFT #5 with temporal variations of AI and RSS_spectra. It is confirmed that both AI and RSS_spectra have the smallest values at the time of LFT #5. For the seismograms obtained in the six days when the seven LFTs associated with the VLFEs were detected, both the AI and RSS_spectra are obviously small in the seven windows, including that of LFTs #1–7, compared with the rest of the seismograms as expected (Fig. 3). It must be noted that the RSS_spectra of LFT #1 is relatively large possibly due to the smallest signal levels (Figure S1 and S3). LFT #6, which is more depleted in the low (~ 1 Hz) frequency components than the others (Figure S3) and is slightly deviated from the others in terms of peak amplitude distribution (Figure S2), has larger AI and RSS_spectra. In this study, we excluded these two events to define the thresholds of RSS_spectra and AI for making LFT detection more conservative. As a result, we set the thresholds as 0.675 and 0.17 for AI and RSS_spectra, respectively based on the AI and RSS_spectra for LFT#2–5 and #7 (Fig. 3).

Although it is expected that AI of SRE-A would be as small as those of LFTs, judging from closeness of the epicenters of SRE-A to that of VLFE #5, its AI is no smaller than the criteria (Fig. 3). Instead, we detected another SRE (SRE-B; M2.7) showing AI smaller than the threshold of LFT detection. Appearance of its seismograms and characteristics of PSDs is similar to those of SRE-A (Figs. 1, S1, S2 and S3), indicating that SRE-B is a regular earthquake located very close to the sources of the LFTs. As to the seismogram of a remote earthquake, RSS_spectra is smaller, but AI is larger than the thresholds (Fig. 3).

Therefore, we can distinguish LFTs from local regular earthquakes and remote earthquakes by using these two quantities. During the six days, there is a seismogram satisfying the criteria of the LFT detection as indicated by a triangle in Fig. 3. The corresponding record appears in Fig. 2 as an event at ~ 10 min before LFT #5. The newly detected event is similar to that of LFT #5 in the seismograms and it can be regarded as an LFT. There are a few events satisfying the LFT-detection threshold of RSS_spectra but not AI (e.g., events at 87 min and 100 min in Fig. 2). Slightly larger AI but acceptably small RSS_spectra of these events indicate that these events are LFTs having different source locations from the group of LFTs that we have identified here.

Newly detected LFTs

By inspecting continuous OBS waveforms based on two parameters, AI and RSS_spectra, we identified 131 LFTs (Figure S4), which are other than the events associated with the known VLFEs. The newly identified LFTs have similar AI and RSS_spectra (Figure S4) and waveform characteristics (Figure S5) with the known LTFs. For most of the events, the windows fulfilling the criteria are isolated, but sometimes, two successive windows satisfy the thresholds. However, both AI and RSS_spectra were not small enough in three or more successive windows. This suggests that the duration of LFTs detected here are not significantly larger than 60 s, that is, twice the window length. This result is consistent with the average duration of the LFTs in the northern Japan Trench (44 s) reported by Nishikawa et al. (2019).

As we define RSS_spectra such that the similarity of the absolute PSDs to that of LFT #5 is evaluated, the detected events should have a similar size to that of LFT #5 as clearly recorded by the OBSs. With the present threshold using the RSS_spectra defined here, the LFT events of different event magnitudes would be missed, if they exist. Here we discuss a possibility of missing events by the proposed method applied to our OBS records. The smaller events are difficult to identify using the other criteria, AI, as they require large S/N among all the five OBS stations. Therefore, we examined the PSDs of all the events larger than LFT #5 to detect the possible large LFT events. Here, we measure magnitudes of the events by averaging the power in the 2–4 Hz frequency range. Among the events having acceptably small AI, there are only few that are larger than LFT #5, which is regarded as a template of our LFT search (Figure S6). Most of them, including SRE-B, have steeper slopes of PSD than LFT #5 indicating that these are regular earthquakes rich in high-frequency content. Nevertheless, we detected a small number of large events with a small PSD slope, relatively rich in low-frequency content. Waveforms of these events resemble those of LFT #5, except for one (d in Figure S6) corresponding to a P-coda part of a remote M 3.8 regular earthquake. These low-frequency events may be LFTs slightly larger than that of LFT #5. Based on the inspection, we regard that LFT #5 is the largest LFT in the area, and missing LFTs larger than that of LFT #5 does not have a significant impact on the discussion on the identified LFTs during our OBS observations.

Discussion

Since our method of searching for LFTs relies on the similarities of the spatial pattern of the observed seismograms, it is expected that the sources of all the detected LFTs must be concentrated within a small area including those accompanied by the seven VLFEs that are used as references. Notably, the signal amplitude distribution of the SRE-B resembles those of the LFTs (Figure S2), and thus, ensures that the AI of SRE-B is as small as the AIs of the LFTs (Fig. 3). Since the similarity of the amplitude variations requires the closeness of the hypocenters as well as of the focal mechanisms, our observation suggests that the detected LFTs are the thrust faulting events in the vicinity of the SRE-B, a regular interplate earthquakes.

We relocated the SREs around SRE-B by P-wave arrivals at five OBS stations to confirm how their epicenter locations and AI values are correlated. As a result, the AIs of the SREs other than SRE-B were significantly larger than that of the threshold for the LFT detection (Figure S7), except one SRE (SRE-B’), which belongs to the sequence of SRE-B, considered as re-rupture of the identical source area for SRE-B. Based on the relocated epicenters, the SREs with AIs larger than the LFT detection threshold are distant from SRE-B by more than ~ 5 km. This suggests that we can differ among epicenter locations using AI with resolution of ~ 5 km and that newly detected LFTs occurred within ~ 5 km from regular interplate earthquakes (SRE-B and SRE-B’). Our result confirms the close collocation of LFTs and the regular occurrence of earthquakes along the Japan Trench subduction zone. In contrast, such coexistence of LFTs and regular earthquakes is rarely observed in the Nankai subduction zone (e.g., Obara and Kato, 2016; Takagi et al., 2019; Uchida et al., 2020), while a regular earthquake was detected close to the VLFE region off the Kii Channel (Takemura et al., 2019).

Figure 4 shows the temporal variation in the detected number of LFTs over an interval of 15 days. The LFTs occurred continuously throughout the observation period; however, we see fluctuations in the number of LFTs. There are two troughs of counts around 30 days and 130 days from the beginning of the observation. We tried to detect any similarities to the present LFT activity during 2016–2018 (Nishikawa et al., 2019) in terms of the temporal variations. For comparison, we selected the LFTs located close to our OBS array from the catalog of Nishikawa et al. (2019) by selecting the LFTs in the area marked by a rectangle in Fig. 1a. Interestingly, the recent LFT activity also showed evident temporal fluctuation with a periodicity of approximately 60–100 days (Fig. 4), which is similar to that of the LFTs in 2011. To examine the significance of the periodicity, we calculated the Schuster p-value (Ader and Avouac, 2013), the probability that a given periodicity is observed from a sequence without periodicity by chance (Figure S8). We observed statistically significant periodicities in the LFTs cataloged by Nishikawa et al. (2019) (Figure S8). From the statistical significance, the possible range of the period is 60–100 days. The LFTs in 2011 also exhibit a decrease in p-value in the similar period range, but the value is not sufficiently small. This is possibly because of the short data period, 193 days, which is much shorter than that of Nihiskawa's catalog (720 days). However, we suggest that LFT-activity preserves a similar pattern in temporal fluctuation from just after the Tohoku-Oki earthquake until 2016–2018. The temporal invariance in the fluctuation period probably show that it is controlled not by the rate of the postseimic slip that decay in the ~ 7 years but by structure near the plate interface. A possible reason for the temporal variations of the LFT-activity is the acceleration and deceleration of the interplate slow slip associated with similar slow slip events such as in Cascadia (Dragert et al., 2004, Rogers et al., 2003) and southwestern Japan (Obara and Ito, 2005). Since the activities of the SREs are considered good indicators of the in situ fault slip rate (e.g., Uchida and Matsuzawa, 2013), we compared them (Fig. 4). During either period, immediately after and more than five years after the Tohoku-Oki earthquake, the SREs and VLFEs tend to occur during the periods of increased LFT activities; however, high LFT activities do not necessarily accompany SREs and VLFEs. The activities of the identified SREs and VLFEs, which are less frequent than those of the LFTs, may be less sensitive to the small-sized slow slip events than those of the LFTs. LFTs can be better indicators to monitor the change in rate of the aseismic slip on the plate interface owing to their higher activity than those of SREs and VLFEs.

Conclusions

We detected several LFTs immediately after the 2011 Tohoku-Oki earthquake in the northern periphery of its aftershock area by temporal OBS observations. Some of the discovered LFTs occurred simultaneously with the VLFEs detected by onshore broadband seismic observations; however, the LFT activity occurred almost continuously throughout the ~ 6 months study period with temporal variation in the strength of the activity. The duration of the identified LFTs is estimated to be less than 60 s, which is consistent with the reported duration for the recent LFTs in the area. These LFTs are considered to occur in the vicinity of a sequence of small repeating earthquakes, which are regular interplate earthquakes. The pattern of the temporal fluctuation of the LFT activity in 2011 resembles that of LFTs during 2016–2018, suggesting that frequent small-scaled slow slip events have repeatedly occurred in intervals of 60–100 days since

2011. These similarities indicate that event duration and temporal variation of the activities have been stable through the postseismic period suggesting structural control of the activity interval. Not all the LFT activities were accompanied by SRE and/or VLFE activities, suggesting that the activities of the LFTs may be more sensitive to small aseismic slip events. Near-field OBS observations by cabled systems as well as pop-up type instruments above the megathrust zone are important to clarify the nature of slow deformation in a shallow subduction zone.

Abbreviations

LFT: Low-frequency tremor

SRE: Small repeating earthquake

VLFE: Very low frequency earthquake

Declarations

Ethics approval and consent to participate

Not applicable.

Consent for publication

Not applicable.

Availability of data and materials

The OBS data used in this article are available online (Now we prepared them in Zenodo).

Competing interests

The authors declare no competing interests.

Funding

This work was supported by JSPS KAKENHI (23900002, 26000002, 17KK0081, and 19H05596).

Authors' contributions

Data analysis and manuscript preparation were carried out mainly by HT. RH, TM, and NU supervised the study at all stages. YO, MS, and SS participated in the design of the study and discussion. All authors read and approved the final manuscript.

Acknowledgements

We thank the captain, crews, and scientists on the Kaiko Maru No. 7 and R/V Hakuho Maru (JAMSTEC) for the acquisition of the ocean bottom seismometer data in the cruise KH11–09. We would like to thank Editage (www.editage.jp) for English language editing. Some figures were created using the Generic Mapping Tools (Wessel & Smith, 1991).

References

1. Ader, T. J., Avouac, J.-P. (2013) Detecting periodicities and declustering in earthquake catalogs using the Schuster spectrum, application to Himalayan seismicity. Earth Planet Sci Lett, 377-378:97-105. https://doi.org/10.1016/j.epsl.2013.06.032
2. Baba, S., Takeo, A., Obara, K., Matsuzawa, T., Maeda, T. (2020) Comprehensive detection of very low frequency earthquakes off the Hokkaido and Tohoku Pacific coasts, Northeastern Japan. J Geophys Res, 125:e2019JB017988. doi:10.1029/2019JB017988
3. Dragert, H., Wang, K., Rogers, G. (2004) Geodetic and seismic signatures of episodic tremor and slip in the northern Cascadia subduction zone. Earth Planet Sci Lett, 56:1143-1150. doi:10.1186/BF03353333
4. Frank, W. B., Shapiro, N. M., Husker, A. L., Kostoglodov, V., Romanenko A., Campillo M. (2014) Using systematically characterized low-frequency earthquakes as a fault probe in Guerrero, Mexico, J Geophys Res, 119:7686-7700, doi:10.1002/2014JB011457.
5. Ghosh, A., Huesca-Pérez, E., Brodsky, E., Ito, Y. (2015) Very low frequency earthquakes in Cascadia migrate with tremor. Geophys Res Lett, 42, 3228-3232. doi:10.1002/2015GL063286
6. Hirata, N., Matsu'ura, M. (1987) Maximum-likelihood estimation of hypocenter with origin time eliminated using nonlinear inversion technique, Phys Earth Planet Inter 47:50-61. doi:10.1016/0031-9201(87)90066-5
7. Ide, S. (2008) A Brownian walk model for slow earthquakes. Geophys Res Lett 35:L17301. doi:10.1029/ 2008GL034821
8. Ide, S. (2019) Detection of low-frequency earthquakes in broadband random time sequences: Are they independent events? J Geophys Res Solid Earth 124:8611-8625. doi:10.1029/2019JB017643
9. Ito, Y., Hino, R., Suzuki, S. Kaneda, Y. (2015) Episodic tremor and slip near the Japan Trench prior to the 2011 Tohoku-Oki earthquake, Geophys Res Lett, 42:1725-1731. doi:10.1002/2014GL062986
10. Kaneko, L., Ide, S., Nakano, M. (2018) Slow earthquakes in the microseism frequency band (0.1–1.0 Hz) off Kii Peninsula, Japan. Geophys Res Lett 45(6):2618-2624. doi:10.1002/2017GL076773
11. Katakami, S., Ito, Y., Ohta, K., Hino, R., Suzuki, S., Shinohara, M. (2018) Spatiotemporal variation of tectonic tremor activity before the Tohoku-Oki Earthquake. J Geophys Res Solid Earth 123:9676-9688. doi:10.1029/2018JB016651
12. Matsuzawa, T., Asano, Y., Obara, K. (2015) Very low frequency earthquakes off the Pacific coast of Tohoku, Japan. Geophys Res Lett 42:4318-4325. doi:10.1002/2015GL063959

13. Nishikawa, T., Matsuzawa, T., Ohta, K., Uchida, N., Nishimura, T., Ide, S. (2019) The slow earthquake spectrum in the Japan Trench illuminated by the S-net seafloor observatories. Science 365(6455):808-813. doi:10.1126/science.aax5618
14. Obana, K., Kodaira, K. (2009) Low-frequency tremors associated with reverse faults in a shallow accretionary prism. Earth Planet Sci Lett 287:168-174. doi:10.1016/j.epsl.2009.08.005
15. Obara, K. (2002) Nonvolcanic deep tremor associated with subduction in southwest Japan. Science 296(5573):1679-1681. doi:10.1126/science.1070378
16. Obara, K., Y. Ito (2005) Very low frequency earthquakes excited by the 2004 off the Kii peninsula earthquakes: A dynamic deformation process in the large accretionary prism, Earth Planets Space 57:321-326. doi:10.1186/BF03352570
17. Obara, K., Kato, A. (2016) Connecting slow earthquakes to huge earthquakes, Science 353:253-257. doi:10.1126/science.aaf1512
18. Ohta, K., Ito, Y., Hino, R., Ohyanagi, S., Matsuzawa, T., Shiobara, H., Shinohara, M. (2019) Tremor and inferred slow slip associated with afterslip of the 2011 Tohoku earthquake. Geophys Res Lett 46:4591-4598. doi:10.1029/ 2019GL082468
19. Rogers, G., Dragert, H. (2003) Episodic tremor and slip on the Cascadia subduction zone: The chatter of silent slip. Science 300(5627):1942-1943. doi:10.1126/science.1084783
20. Takagi, R., Uchida, N., Obara, K. (2019) Along-strike variation and migration of long-term slow slip events in the western Nankai subduction zone, Japan. J Geophys Res Solid Earth 124:3853-3880. doi:10.1029/2018JB016738
21. Takemura, S., Noda, A., Kubota, T., Asano, Y., Matsuzawa, T., Shiomi, K. (2019) Migrations and clusters of shallow very low frequency earthquakes in the regions surrounding shear stress accumulation peaks along the Nankai Trough. Geophys Res Lett 46(21):830–11,840. doi:10.1029/2019GL084666
22. Tanaka, S., Matsuzawa, T., Asano, Y. (2019) Shallow low-frequency tremor in the northern Japan Trench subduction zone. Geophys Res Lett 46:5217-5224. doi:10.1029/ 2019GL082817
23. Todd, E. K., Schwartz, S. Y., Mochizuki, K., Wallace, L. M., Sheehan, A. F., Webb, S. C., Williams, C. A., Nakai, J., Yarce, J., Fry, B., Henrys, S., Ito, Y. (2018) Earthquakes and tremor linked to seamount subduction during shallow slow slip at the Hikurangi Margin, New Zealand. J Geophys Res Solid Earth 123:6769-6783. doi:10.1029/2018JB016136
24. Toh, A., Obana, K., Araki, E. (2018) Distribution of very low frequency earthquakes in the Nankai accretionary prism influenced by a subducting-ridge. Earth Planet Sci Lett 482:342-356. doi:10.1016/j.epsl.2017.10.062
25. Uchida, N., Matsuzawa, T. (2013) Pre- and postseismic slow slip surrounding the 2011 Tohoku-oki earthquake rupture. Earth Planet Sci Lett 374:81-91. doi:10.1016/j.epsl.2013.05.021
26. Uchida, N., Takagi, R. Asano, Y. Obara, K. (2020) Migration of shallow and deep slow earthquakes toward the locked segment of the Nankai megathrust. Earth Planet Sci Lett 531:115986. doi:10.1016/j.epsl.2019.115986

27. Yamashita, Y., Yakiwara, H., Asano, Y., Shimizu, H., Uchida, K., Hirano, S., Umakoshi, K., Miyamachi, H., Nakamoto, M., Fukui, M., Kamizono, M., Kanehara, H., Yamada, T., Shinohara, M., Obara, K. (2015) Migrating tremor off southern Kyushu as evidence for slow slip of a shallow subduction interface. Science, 348(6235):676-679. doi:10.1126/science.aaa4242

Figures

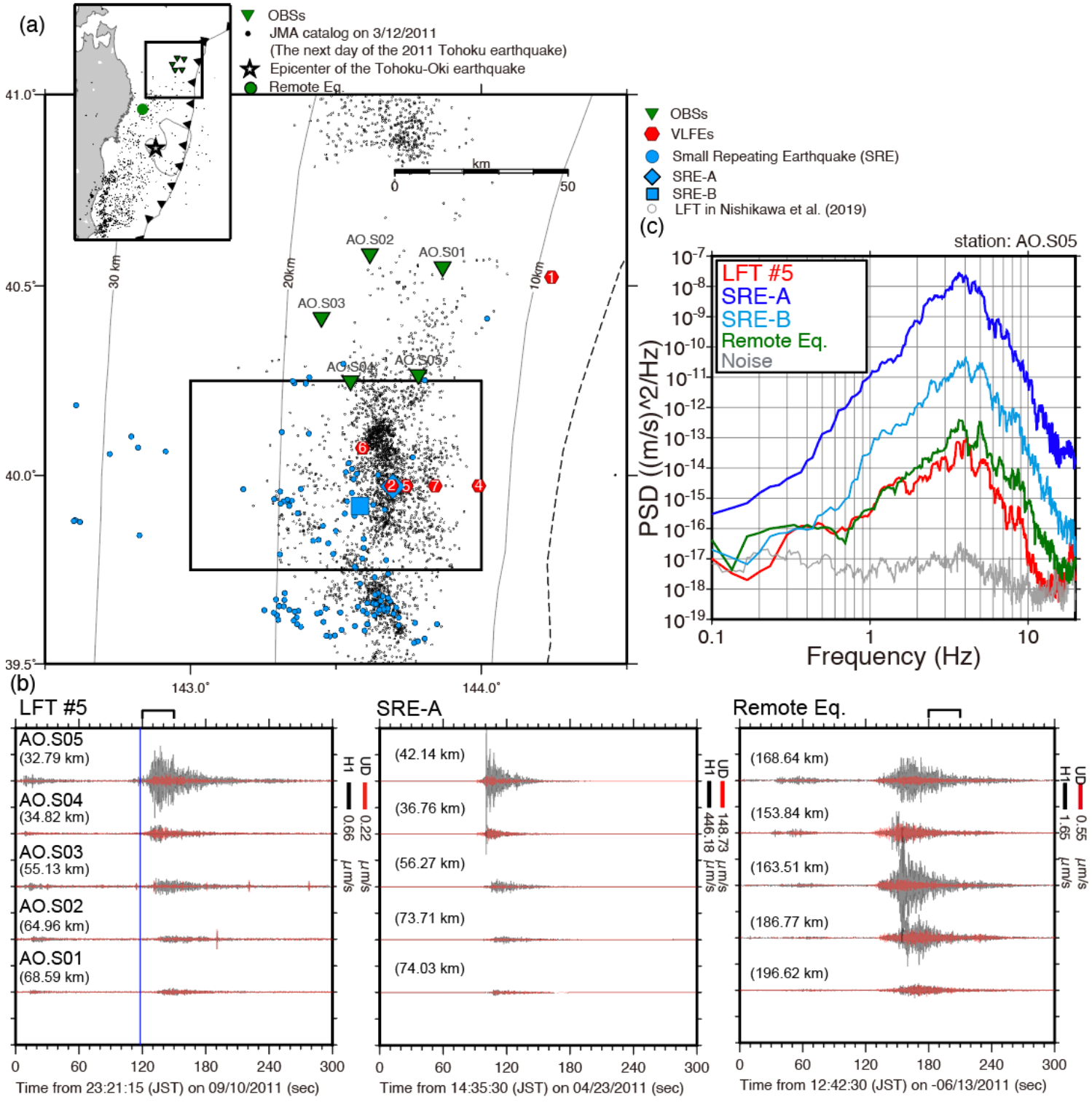

Figure 1

Location map of OBSs and known VLFEs, and characteristics of LFTs observed by the OBSs. (a) OBS stations and VLFE epicenter map. Reverse triangles and hexagons are OBSs and VLFEs, respectively. Blue circles are small repeating earthquakes (SREs) that occurred between April 10 to October 25, 2011. Diamond (SRE-A) is an SRE (M 3.9) whose seismograms are compared to those of the LFTs. Square (SRE-B) is SRE (M2.7) which is considered to have closest hypocenter to LFTs. The depth contours of the plate boundary (Nakajima and Hasegawa, 2006) are shown by black lines. Dashed line indicates the trench axis of the Japan Trench. Black dots in the inset map on the upper left are Japan Meteorological Agency (JMA) epicenters of regular earthquakes on 12 March, 2011 defining the aftershock area of the 2011 Tohoku-Oki earthquake, whose epicenter is shown by a star. (b) Filtered (2–4 Hz) seismograms during LFT #5, SRE-A, B and a remote earthquake (M 3.4) whose location is shown in the left top inset of (a) as a green circle. Vertical and horizontal records are shown by red and black traces, respectively. Epicentral distances are shown in parentheses. Vertical blue line shows the origin time of the VLFE #5. (c) Power spectra of the LFT, the SRE, and the remote earthquake are shown in (b). Horizontal records at AO.S05 in the time window indicated by brackets in (b) are used. Background noise is taken from a window at 30 min before the origin time of VLFE #5. Note: The designations employed and the presentation of the material on this map do not imply the expression of any opinion whatsoever on the part of Research Square concerning the legal status of any country, territory, city or area or of its authorities, or concerning the delimitation of its frontiers or boundaries. This map has been provided by the authors.

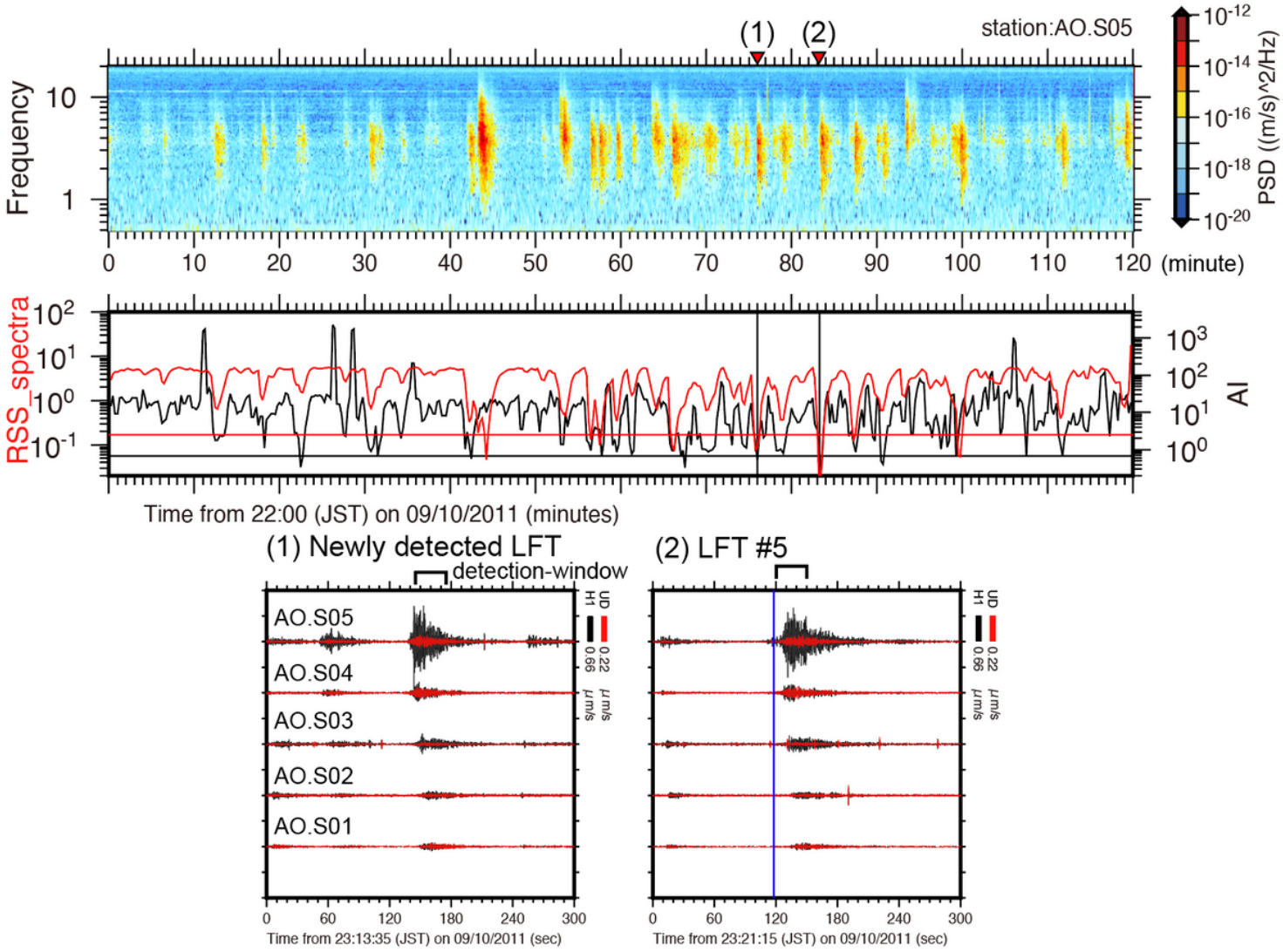

Figure 2

Two-hour spectrogram of the horizontal components at AO.S05 (top), with temporal variation of AI and RSS_spectra (middle), and seismograms of two identified LFTs, (1) and (2), (bottom). Horizontal red and black lines in the middle panel show detection threshold of RSS_spectra and AI, respectively. Vertical and horizontal component records are shown by red and black traces, respectively.

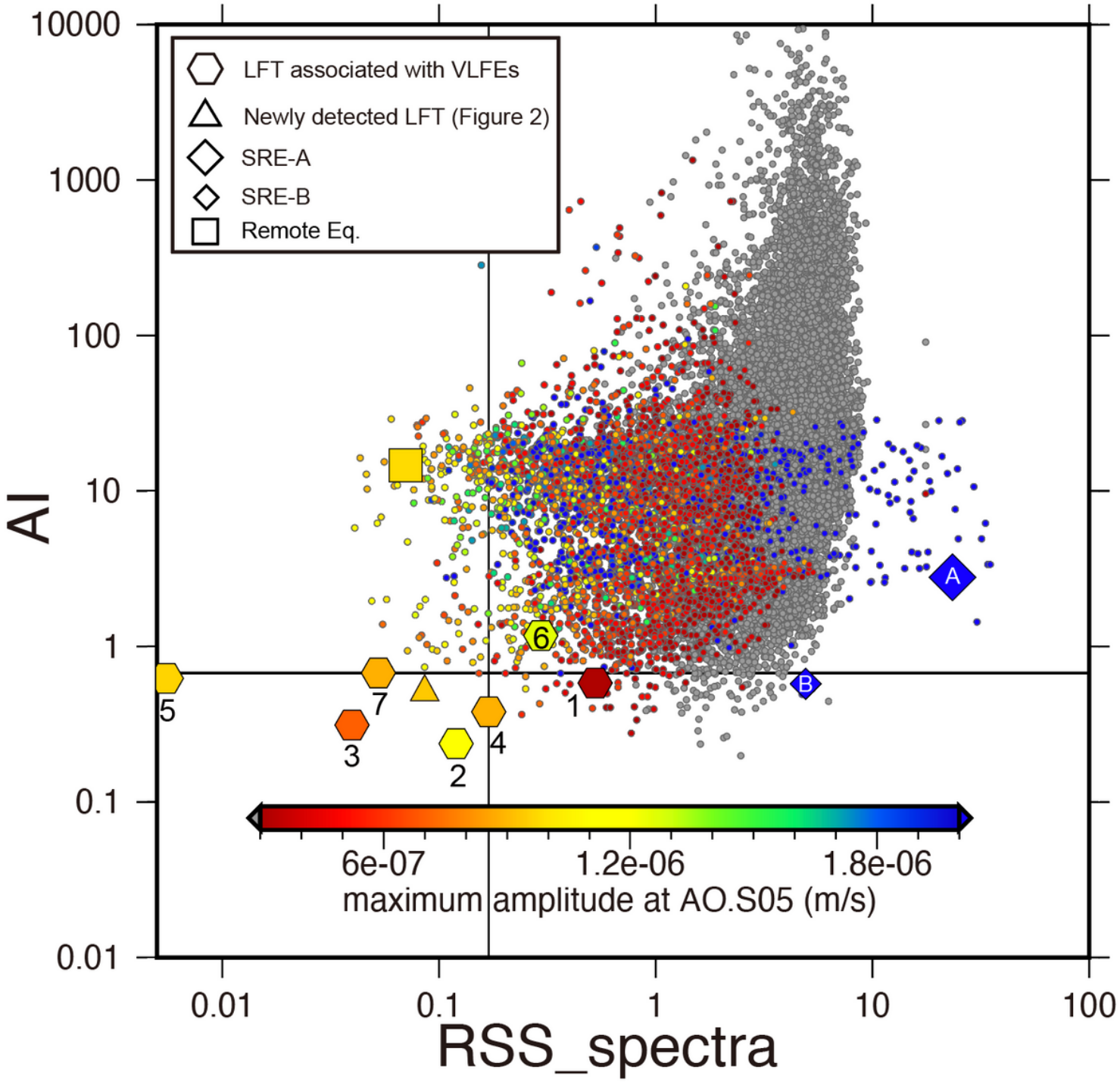

Figure 3

Results of waveform classification using AI and RSS_spectra for the six days, when the reported VLFEs occurred. Hexagons are LFT #1–7, a diamond is SRE, and a square is the remote earthquake. Symbol colors show the maximum amplitude at station AO.S05 at the corresponding time window. Thresholds of RSS_spectra and AI are shown by vertical and horizontal lines, respectively. AI and RSS_spectra calculated for SRE-A and a remote earthquake are also shown, although these earthquakes happened on different days. RSS_spectra of LFT #5 is not exactly zero in the figure, because the time window including LFT #5 in the event searching is slightly different from that for the reference PSD calculation.

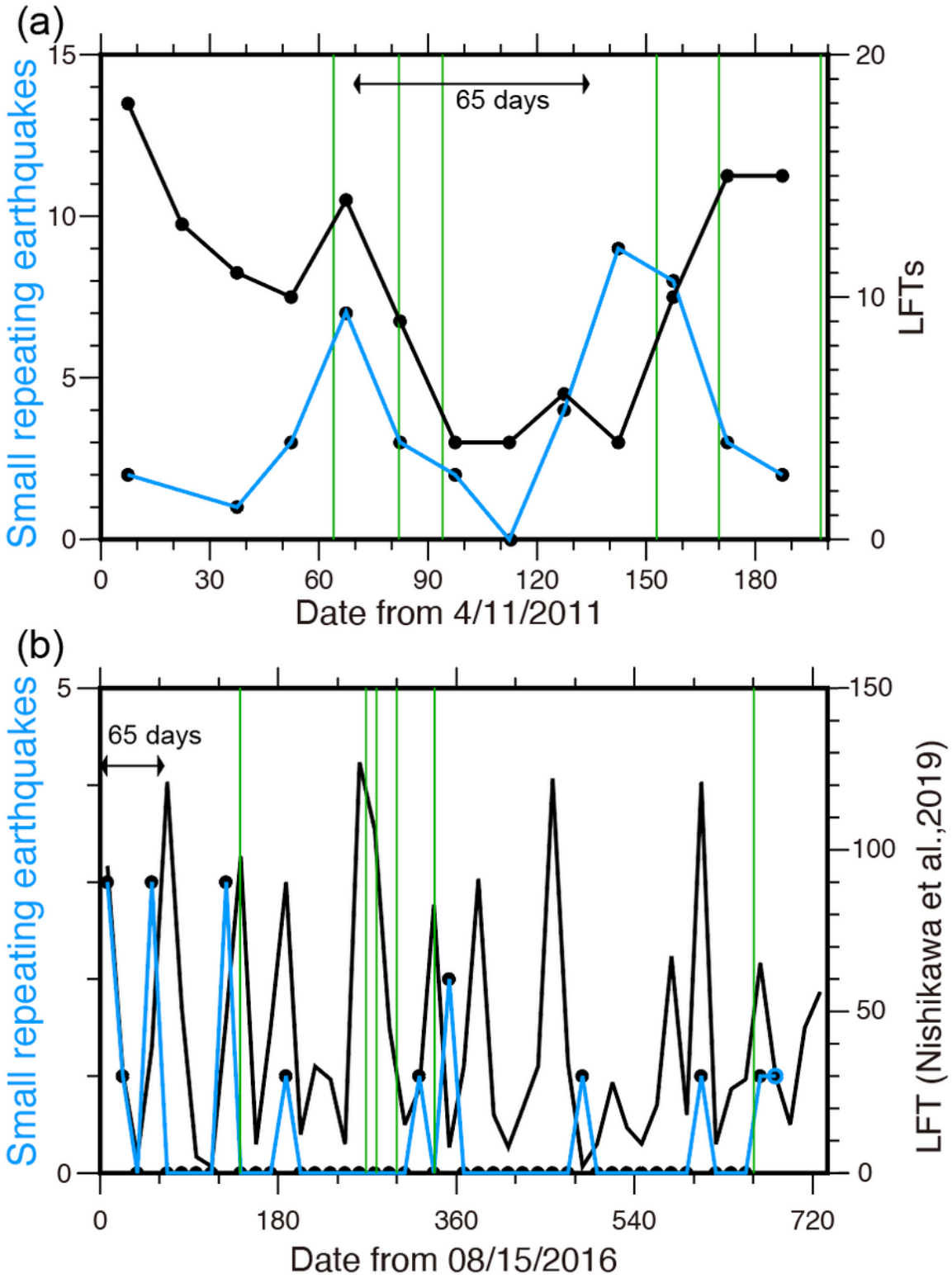

Figure 4

Numbers of detected LFTs and SREs in a 15-days interval. (a) For the period of the temporal OBS observations during April 10 to October 25 in 2011. Black and blue lines are for the LFTs and SREs, respectively. Green lines indicate the occurrence times of the VLFEs (Matsuzawa et al.,2015). (b) For the period from Aug. 15, 2016 to Aug. 14, 2018 (Nishikawa et al., 2019). Double-headed arrows in (a) and (b) show the period giving the lowest Schuster p-value for the LFTs activities during 2016 and 2018.

Supplementary Files

This is a list of supplementary files associated with this preprint. Click to download.

- graphicalabstract.png
- EPSAdditionalfiletakahashisubmit.pdf